# Identification of new transitions feeding the high-spin isomers in $^{139}$Nd and $^{140}$Nd nuclei

A. Vancraeyenest, C. Petrache, D. Guinet, P. T. Greenlees, U. Jakobsson, R. Julin, S. Juutinen, S. Ketelhut, M. Leino, M. Nyman, et al.

# Identification of new transitions feeding the high-spin isomers in $^{139}$Nd and $^{140}$Nd nuclei

A. Vancraeyenest,[1,2] C. M. Petrache,[3] D. Guinet,[1] P. T. Greenlees,[4] U. Jakobsson,[4] R. Julin,[4] S. Juutinen,[4] S. Ketelhut,[4] M. Leino,[4] M. Nyman,[4] P. Peura,[4] P. Rahkila,[4] P. Ruotsalainen,[4] J. Saren,[4] C. Scholey,[4] J. Sorri,[4] J. Uusitalo,[4] P. Jones,[4,5] C. Ducoin,[1] P. Lautesse,[1] C. Mancuso,[1] N. Redon,[1] O. Stezowski,[1] P. Désesquelles,[3] R. Leguillon,[3] A. Korichi,[3] T. Zerrouki,[3] D. Curien,[6] and A. Takashima[7]

[1]*IPNL, Université de Lyon, Université Claude Bernard Lyon 1, and CNRS/IN2P3, F-69622 Villeurbanne, France*

[2]*LPSC, Université Joseph Fourier, INP, and CNRS/IN2P3, F-38026 Grenoble, France*

[3]*Centre de Spectrométrie Nucléaire et de Spectrométrie de Masse, Université Paris-Sud and CNRS/IN2P3, Bât. 104-108, F-91405 Orsay, France*

[4]*Department of Physics, University of Jyväskylä, Jyväskylä FIN-40014, Finland*

[5]*iThemba LABS, National Research Foundation, P.O. Box 722, Somerset West 7129, South Africa*

[6]*Departement de Recherches Subatomiques, Institut Pluridisciplinaire Hubert Curien, DRS-IPHC, 23 rue du Loess, Boîte Postale 28, F-67037 Strasbourg, France*

[7]*Department of Physics, Osaka University, Toyonaka, Osaka 560-0043, Japan*

(Received 31 January 2013; revised manuscript received 10 May 2013; published 10 June 2013)

The population of the high-spin isomers in $^{139}$Nd and $^{140}$Nd was investigated using the $^{96}$Zr($^{48}$Ca,$xn$) reaction and the JUROGAM + RITU + GREAT setup employing the recoil decay tagging technique. Three transitions feeding the $23/2^+$ isomer in $^{139}$Nd and two transitions feeding the $20^+$ isomer in $^{140}$Nd were identified. The newly observed transitions allowed the excitation energy of the isomer to be established in $^{139}$Nd and to assign configurations to the states and bands deexcited by the observed transitions in both nuclei.

DOI: 10.1103/PhysRevC.87.064303 PACS number(s): 21.10.Re, 23.20.Lv, 23.35.+g, 27.60.+j

## I. INTRODUCTION

The nuclei around the $N = 82$ shell closure whose configurations can be considered relative to a $^{146}$Gd core are a fertile field of spectroscopic investigations at both low and high spins. At low spins the presence of isomers based on simple particle-hole excitations helps to establish the active quasiparticle configurations in a specific nucleus and to test the suitability of various nuclear potentials, whereas at high spins the combined contribution of neutron holes in the $N = 82$ core and neutron particles in the high-$j$ orbitals above the $N = 82$ gap drives the nuclear shape toward a stable triaxial shape with $\gamma \approx +30^\circ$ [1,2]. The coexistence of different shapes is another phenomenon present in these nuclei. In particular, superdeformed and highly deformed bands have been observed in $^{140}$Nd [3] and $^{138}$Nd [4], coexisting with several triaxial bands [1]. The $^{138}$Nd nucleus is considered to have a triaxial shape at low and medium spins, based on the agreement between the cranked Nilsson-Strutinsky calculations and the multitude of bands reported recently in Ref. [5]. The observation of excited states in the nearly spherical nuclei close to the shell closures is more difficult than the observation of excited states in the well-deformed nuclei due to the presence of isomeric states, which often interrupts and fragments the decay flux. Such a situation is encountered in the weakly deformed Nd nuclei with neutron numbers close to the $N = 82$ shell closure, with irregular sequences of transitions and possible yrast traps. In fact, isomeric states were observed in $^{138}$Nd ($I^\pi = 10^+$, $T_{1/2} = 410$ ns) [6] and $^{140}$Nd ($I^\pi = 7^-$, $T_{1/2} = 600\ \mu$s) [7]. More recently, new experimental data were published for the $^{140}$Nd nucleus, which presents a $20^+$ isomeric state at $E_x = 7.43$ MeV, with a 6-quasiparticle configuration [8]. A lifetime of $T_{1/2} = 1.23(7)$ $\mu$s has been measured in a pulsed-beam experiment performed at the Tandem of IPN, Orsay [9]. This value supports the $20^+$ spin-parity assignment and the interpretation as a spherical configuration that coexists with the surrounding triaxial bands. In the same experiment the delayed components of the transitions below the $19/2^+$ state in $^{139}$Nd were also measured, which indicate the existence of an isomeric state with an apparent half-life of 272(4) ns. The excitation energy of the isomer could not be determined in that experiment due to an unobserved low-energy transition between the isomer and the lower-lying $19/2^+$ state.

However, even though the level schemes of both nuclei were developed up to very high spins, no transitions feeding the isomeric states from higher-lying states were observed. We have therefore performed a dedicated experiment to search for transitions populating the isomeric states. As the lifetimes of the isomers are long enough to employ the recoil-tagging technique, we used the high-efficiency gas-filled recoil mass separator RITU and in addition the high-efficiency arrays JUROGAM II (called JUROGAM in the following) placed at the target position and the GREAT spectrometer placed at the entrance and the focal plane of the RITU separator.

The details of the experimental setup are briefly discussed in Sec. II. The results are presented in Sec. III. The configurations of the different bands are discussed in Sec. IV. Finally, the summary is given in Sec. V.

## II. EXPERIMENTAL DETAILS

High-spin states in $^{139}$Nd and $^{140}$Nd were populated via the $^{96}$Zr($^{48}$Ca,$xn$) reaction at a beam energy of 180 MeV. The target consisted of a self-supporting $^{96}$Zr foil of 735 $\mu$g/cm$^2$ thickness. The $^{48}$Ca beam was provided by the K130 Cyclotron at the university of Jyväskylä, Finland. The $^{139}$Nd and $^{140}$Nd

 

nuclei were the most strongly populated in the reaction, with cross sections of around 200 mb each.

The JUROGAM array placed at the target position was composed of 39 Compton-suppressed Ge detectors: 24 clover detectors and 15 coaxial tapered detectors. The clovers were placed on two rings at 75.5° (12 clovers) and 104.5° (12 clovers) symmetric with respect to 90°, while the tapered detectors were placed on two rings at backward angles of 133.6° (10 detectors) and 157.6° (5 detectors). The GREAT spectrometer around the RITU focal plane was composed of several detector types. A multiwire proportional counter (MWPC) was used to measure the position of the recoils and gave the time reference for the delayed $\gamma$-$\gamma$ coincidences and for the measurement of the time of flight of the recoils between the MWPC and a silicon Double side Silicon Strip Detectors (DSSD) placed downstream of the MWPC. Behind the DSSD was placed a segmented planar Ge detector of 12 cm × 6 cm corresponding to 24 × 12 segments with a thickness of 1.5 cm, used for the measurement of x rays and low-energy $\gamma$ rays. For the measurement of high-energy $\gamma$ rays, a large volume clover with each crystal segmented into four was placed just above the focal plane reaction chamber and two clovers were placed on the right and left sides of the reaction chamber. The JUROGAM array was used for standard coincidence measurements of $\gamma$ rays, while the time-correlated events in JUROGAM and GREAT were used to measure delayed $\gamma$-$\gamma$ coincidences.

The trigger condition for the acquisition of events from either JUROGAM or GREAT was the measurement of a recoil signal in the MWPC in coincidence with at least a $\gamma$ ray in JUROGAM within a time window of [−5 $\mu$s, 10 $\mu$s] with respect to the time reference given by the MWPC. Given the isomer lifetimes of 272 ns in $^{139}$Nd and 1.23 $\mu$s in $^{140}$Nd, and the flight time through RITU of around 650 ns, this time window allowed us to measure the major part of the isomer decays and the delayed $\gamma$-$\gamma$ coincidences. The event rate was around 13 kHz, which was low enough to avoid the overlap between successive events separated on average by 80 $\mu$s. The events were stamped by the Total Data Readout (TDR) data acquisition, and then they were sorted using GRAIN code [10]. The analysis was performed with the GammaWare [11] and Radware [12,13] programs.

A total of $5 \times 10^9$ events was collected. Thanks to the high efficiency of the various $\gamma$-ray arrays, we produced $\gamma$-$\gamma$ matrices for each array, i.e., for JUROGAM at the target position, for the clovers, and for the segmented planar Ge detectors at the focal plane. The lifetime of the isomeric states in the nuclei implanted in the DSSD detector at the focal plane was measured using $\gamma$-time ($\gamma$-$T$) matrices. The clean $\gamma$ rays used to extract the isomer lifetimes were chosen by analyzing the $\gamma$-$\gamma$ matrices between the detectors at the focal plane.

## III. RESULTS

### A. Lifetimes of isomers in $^{138}$Nd, $^{139}$Nd, $^{140}$Nd, and $^{136}$Ce

The relevant parts of the level schemes of $^{139}$Nd and $^{140}$Nd are shown in Figs. 1 and 2, respectively. In the level scheme of $^{139}$Nd are included the band built on the $h_{11/2}$ isomer and three other bands, D1, D2, and Q1, which have decay branches towards the $23/2^+$ isomer or towards the $19/2^+$ state just below it. In the level scheme of $^{140}$Nd are included the two dipole bands D3 and D4 which have a decay branch towards the $20^+$ isomer, as well as the other band, Band 12, which is observed in coincidence with delayed transitions detected at the focal plane. The newly observed transitions, populating the $20^+$ isomeric state in $^{140}$Nd and the $23/2^+$ isomeric state in $^{139}$Nd, are drawn with black (red) arrows and their energies are boxed.

A $\gamma$-$T$ matrix for the clovers of the focal plane is shown in Fig. 3. One can see time spectra of different lengths for the 605-, 665-, and 1071-keV transitions below the $23/2^+$ ($T_{1/2} = 272$ ns) isomeric state in $^{139}$Nd; the 729-, 884-, and 972-keV transitions below the $10^+$ ($T_{1/2} = 0.41$ $\mu$s) isomeric state in $^{138}$Nd; and the 773- and 1028-keV transitions below the $7^-$ ($T_{1/2} = 600$ $\mu$s) isomeric state in $^{140}$Nd.

We have measured the lifetimes of isomeric states in the $^{140}$Nd, $^{139}$Nd, $^{138}$Nd, and $^{136}$Ce nuclei; the results are shown in Table I. The lifetime in each nucleus was deduced from spectra of each individual $\gamma$ ray in the deexcitation cascade below the isomeric state, after proper background subtraction and fit with an exponential decay curve. The $\gamma$ rays used to extract the lifetime of the isomer are indicated in Table I. The present lifetimes are deduced from the analysis (average value of the fitted value) of individual $\gamma$ rays, which is not always the case for the previously reported lifetimes which were extracted from summed spectra of several transitions below the isomeric state. Time spectra of the transitions deexciting the isomeric states and a representative fit are shown in Fig. 4. The lifetime values of the $20^+$ isomer in $^{140}$Nd and of the $23/2^+$ isomer in $^{139}$Nd are in agreement with those reported previously [9]. The lifetime of the $10^+$ isomer in $^{138}$Nd is 370 ± 5 ns, a value significantly lower but yet compatible with the 410 ± 50 ns reported previously [6]. The same is true for the lifetime of the $10^+$ isomer in $^{136}$Ce of 1.9 ± 0.1 $\mu$s, which is significantly lower than the 2.2 ± 0.2 $\mu$s value reported previously [6,14].

### B. Transitions populating the $23/2^+$ isomer in $^{139}$Nd and the $20^+$ isomer in $^{140}$Nd

The main advantage of the JUROGAM + RITU + GREAT setup used in the present experiment was to separate the detection of the prompt $\gamma$ rays populating the isomers at the target position from the detection of the delayed $\gamma$ rays deexciting the isomers with sufficiently long lifetime at the focal plane. We can therefore select very weak prompt $\gamma$ rays produced at the target position by gating on time-correlated $\gamma$ rays delayed by $\geqslant$650 ns. For the identification of the $\gamma$ rays of a specific nucleus we produced $\gamma$-$\gamma$ matrices between the delayed transitions detected by the clovers and the segmented planar detector placed at the focal plane. To search for transitions feeding the isomers we produced $\gamma$-$\gamma$ matrices between JUROGAM and the Ge detectors placed at the focal plane (clovers and the segmented planar).

#### *1. Transitions populating the $20^+$ isomer in $^{140}$Nd*

To obtain the transition above the $20^+$ isomer in $^{140}$Nd, the first step is the focal plane spectrum coming from a $\gamma$-$\gamma$ matrix of the clovers placed at the focal plane by gating on

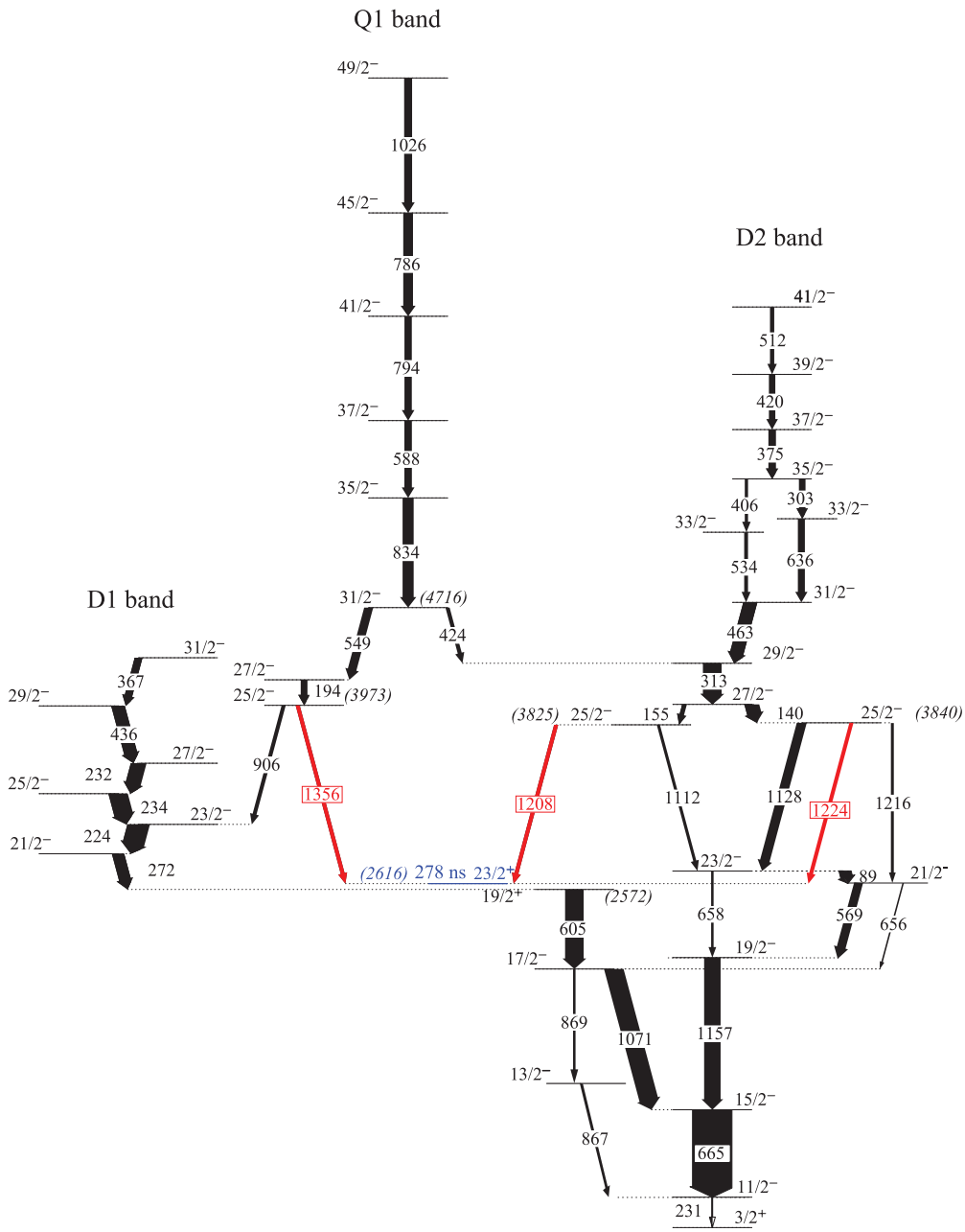


FIG. 1. (Color online) Partial level scheme of $^{139}$Nd in which only selected transitions are drawn (arrow thickness is proportional to intensity), the newly observed transitions are drawn in black (red) and their energies (1356, 1208, and 1224) are boxed [15].

the 868-keV $11^- \rightarrow 9^-$ transition in $^{140}$Nd. The spectrum is dominated by delayed transitions below the $20^+$ isomer in $^{140}$Nd, i.e., 177, 182, 188, 191, 216, 229, 258, 343,433, 437, 506, 695, 728, 773, 840, 868, 991, 1017, and 1028 keV [8].

After a careful analysis of the $\gamma$-$\gamma$ matrix obtained with the focal plane detectors, the second step is then to select the cleanest transitions to extract the prompt-delayed spectra between JUROGAM and the detectors at the focal plane. An example of a prompt spectrum from JUROGAM obtained by gating on selected transitions of $^{140}$Nd measured at the focal plane is shown in Fig. 5.

Most of the transitions present in this spectrum were observed in prompt coincidence with low-lying transitions of $^{140}$Nd [2]. But we observed two new strong transitions of 754 and 1196 keV, which directly connect the previously observed 8186- and 8628-keV states of bands D4 and D3, respectively, to the $20^+$ isomeric state. A new weaker transition of 1088 keV connecting the 8520-keV state of the D4 band with the $20^+$ isomer was also observed. Finally, two new transitions of 233 and 253 keV were placed on top of band D3 and between bands D3 and D4, respectively. We should mention that the placement of the 754- and 1196-keV transitions between the bands D4 and D3 and the $20^+$ isomer was facilitated by the fact that the energies of the lowest states of the two bands were known: a prompt transition of 1541-keV deexciting band D4 towards the $17^-$ state at 6404 keV and one transition of

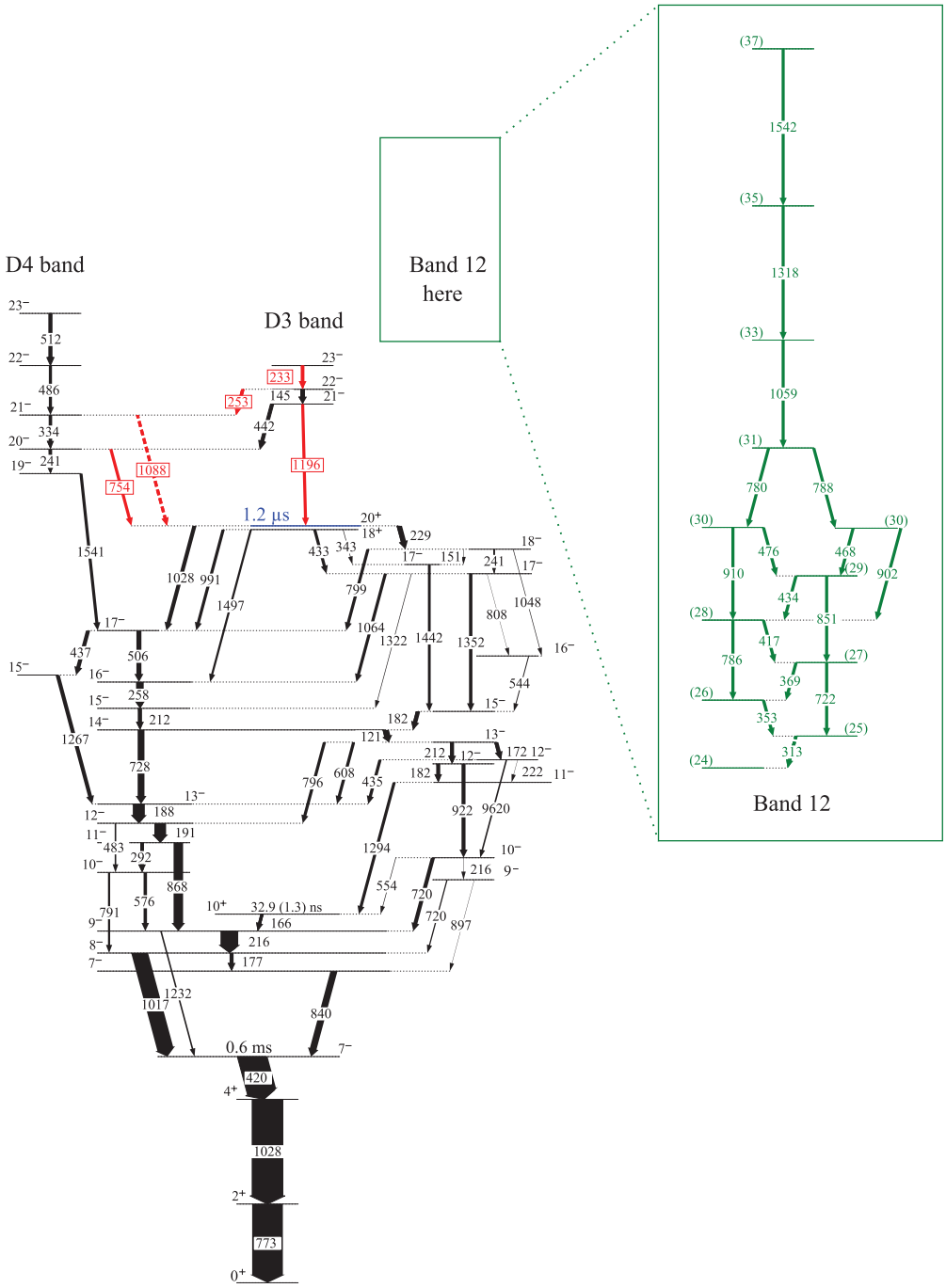


FIG. 2. (Color online) Partial level scheme of $^{140}$Nd in which only selected transitions are drawn with arrows (arrow thickness is proportional to intensity), the newly observed transitions are drawn in black (red) and their energies [754, (1088), 253, 233 and 1196] are boxed. The black (green) transitions named Band 12 have been observed in a previous work [8].

442 keV between the bands D3 and D4 had been identified previously [2].

For Band 12 the situation was more complicated due to the fact that no linking transitions to low-lying states were known. As one can see in Fig. 6, the prompt spectrum in coincidence with delayed transitions of $^{140}$Nd and with transitions of Band 12 above the spin 26 shows all the transitions assigned to Band 12 and the transitions from band D4. It seems that Band 12 is connected to low-lying states through the 600-keV transition. However, the statistics for these weak transitions were not enough to establish the connection of Band 12 with low-lying states.

### 2. *Transitions populating the* $23/2^+$ *isomer in* $^{139}$Nd

The isomer in $^{139}$Nd was known to lie slightly above the $19/2^+$ state at 2572 keV. As only the transitions below the $19/2^+$ state showed a delayed component in the time spectra

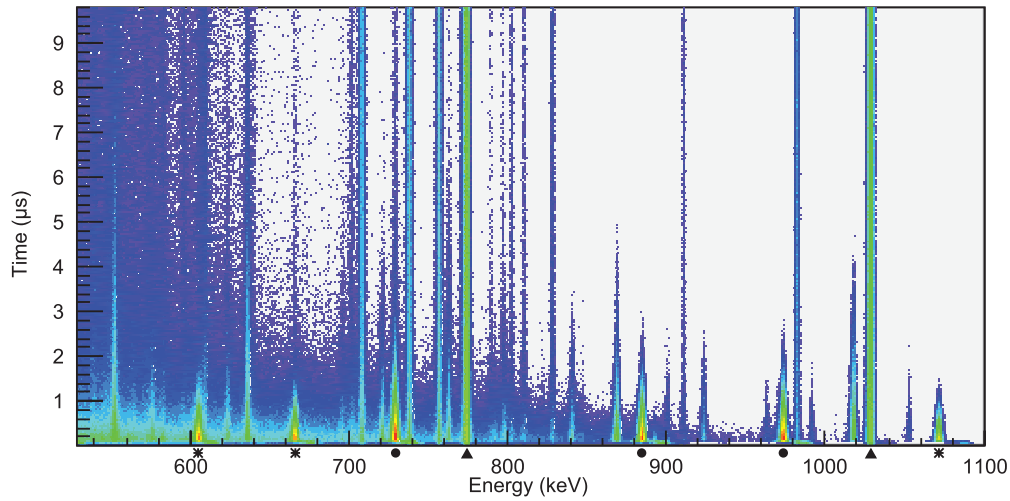


FIG. 3. (Color online) $\gamma$-$T$ matrix for the clovers at the focal plane. The transitions below the isomeric state in $^{138}$Nd are marked with a circle, those in $^{139}$Nd with a star, and those in $^{140}$Nd with a triangle.

[9], it was known that it decays only to the $19/2^+$ state through an unobserved low-energy transition. The prompt spectrum of JUROGAM gated by the delayed 605-, 665-, and 1071-keV transitions below the $23/2^+$ isomer at the focal plane is shown in Fig. 7. One can observe transitions towards the known levels from known excited states of $^{139}$Nd, but can also observe three new high-energy transitions of 1208, 1224, and 1356 keV.

To link the new transitions to the known level scheme of $^{139}$Nd [15], we built prompt $\gamma$-$\gamma$ matrices from the events in JUROGAM gated by delayed transitions detected at the focal plane. Examples of spectra doubly gated by the delayed transitions emitted at the focal plane and prompt transitions detected in JUROGAM are shown in Figs. 8 and 9. One can see in Fig. 8 that the spectrum gated by the 140-keV transition shows the previously known transitions of 313, 375, 424, and 463 keV placed above the $27/2^-$ state at 3982 keV deexcited by the 140-keV transition, but also the new 1224-keV transition deexciting the $25/2^-$ state at 3841 populated by the 140-keV transition. Similarly, in the spectrum shown in Fig. 9 which is gated by the 194-, 549-, and 834-keV transitions one can see the previously known transitions populating the $27/2^-$ state at 4167 keV deexcited by the 194-keV transition, but also the new 1356-keV transition deexciting the $25/2^-$ state at 3973 keV. We can therefore deduce that placing the 1224- and 1356-keV transitions directly below the $25/2^-$ states at 3840 and 3973 keV, respectively, we get the same state at an excitation energy, which we identify with the $23/2^+$ isomer. In addition to these two transitions, we observe a weaker prompt transition of 1208 keV in coincidence with the 155-keV transition, which fits with the energy difference between the $25/2^-$ state at 3825 keV and the $23/2^+$ isomer at 2616 keV. We therefore consider to have established the energy of the $23/2^+$ isomer in $^{139}$Nd at 2616 keV, which implies the existence of an unobserved $\gamma$ ray of 45 keV towards the $19/2^+$ state at 2572 keV.

## IV. DISCUSSION

The level structure of the $^{139}$Nd and $^{140}$Nd nuclei with 60 protons and 79–80 neutrons results from the combination of 10 proton particles on top of the $Z = 50$ major shell, or alternatively 4 proton holes in the $Z = 64$ subshell and 2–3 neutron holes in the $N = 82$ major shell. For low and medium spins, the nucleus is expected to have a small deformation, $\epsilon_2 \sim 0.10$–$0.15$. It is thus convenient to express the single-particle states in terms of $j$-shell quantum numbers. The lowest proton configuration has 4 proton holes in the $\pi g_{7/2}$ and $\pi d_{5/2}$ orbitals which interact and are strongly mixed. Higher angular momenta from proton configurations can be obtained by exciting 1 or 2 protons from the $\pi g_{7/2}$ and $\pi d_{5/2}$ orbitals

TABLE I. Lifetimes of isomers in various nuclei populated in the reaction. The different columns indicate the nucleus, spin-parity, the energy of the $\gamma$ ray used for deducing the lifetimes, the present results (obtained by averaging the extracted value from each $\gamma$ spectrum of the left-hand column), the previous reported results, and the reference article.

| Nucleus | Spin $I^\pi$ | Energies of $\gamma$ (keV) | $T_{1/2}$ | | |
|---|---|---|---|---|---|
| | | | Present work | Previous works | Ref. |
| $^{140}$Nd | $20^+$ | 229, 258, 343, 433, 991, 1352, 1442, and 1497 | $1.2 \pm 0.1$ $\mu$s | $1.23 \pm 0.07$ $\mu$s | [9] |
| $^{139}$Nd | $23/2^+$ | 605, 665, and 1071 | $278 \pm 2$ ns | $272 \pm 4$ ns | [9] |
| $^{138}$Nd | $10^+$ | 68, 521, 884, and 972 | $370 \pm 5$ ns | $410 \pm 50$ ns | [6] |
| $^{136}$Ce | $10^+$ | 552, 623, 762, and 1052 | $1.9 \pm 0.1$ $\mu$s | $2.2 \pm 0.2$ $\mu$s | [6,14] |

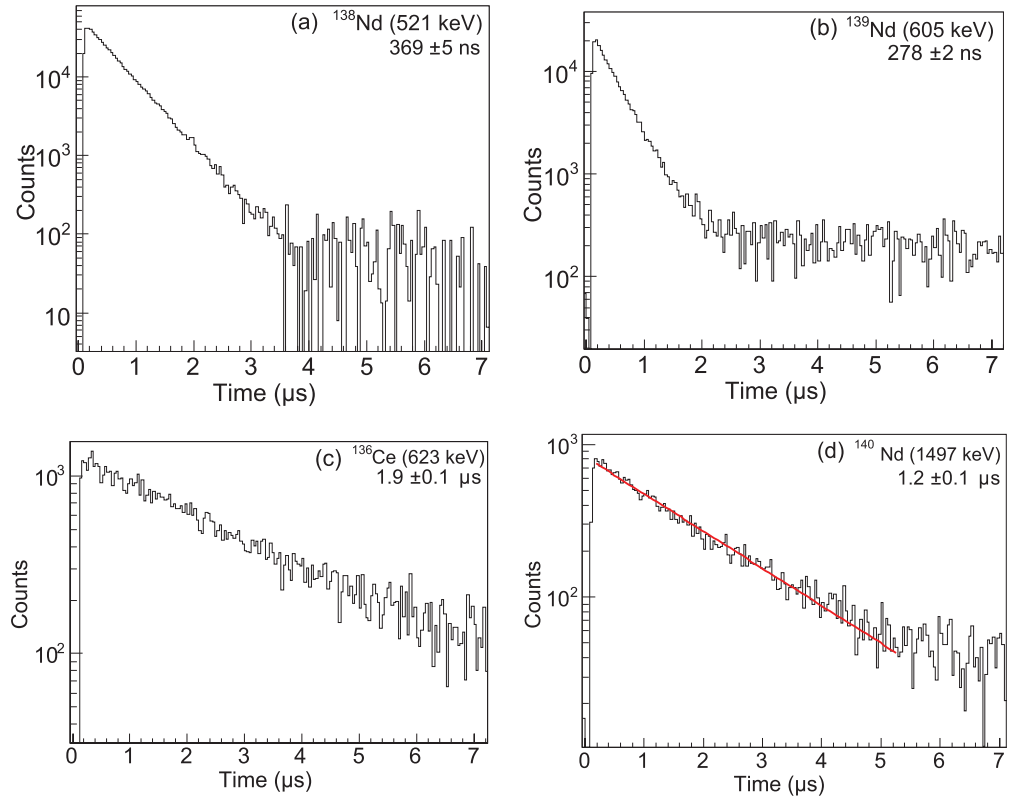


FIG. 4. (Color online) Time spectra extracted from $\gamma$-$T$ matrix at the focal plane: (a) 521-keV transition deexciting the $10^+$ isomer in $^{138}$Nd, (b) 605-keV transition deexciting the $23/2^+$ isomer in $^{139}$Nd, (c) 623-keV transition deexciting the $10^+$ isomer in $^{136}$Ce, and (d) 1497-keV transition deexciting the $20^+$ isomer in $^{140}$Nd [the associated fit is shown in black (red)].

to the $\pi h_{11/2}$ orbital. The lowest neutron configuration has 2-3 holes in the $\nu d_{3/2}$ and $\nu s_{1/2}$ orbitals which interact and are strongly mixed. Higher angular momenta from neutron configurations can be obtained by exciting 1 or 2 neutrons from the $\nu h_{11/2}$ orbital into the $\nu d_{3/2}$ and $\nu s_{1/2}$ orbitals, all lying below the $N = 82$ shell gap. Many more excited states

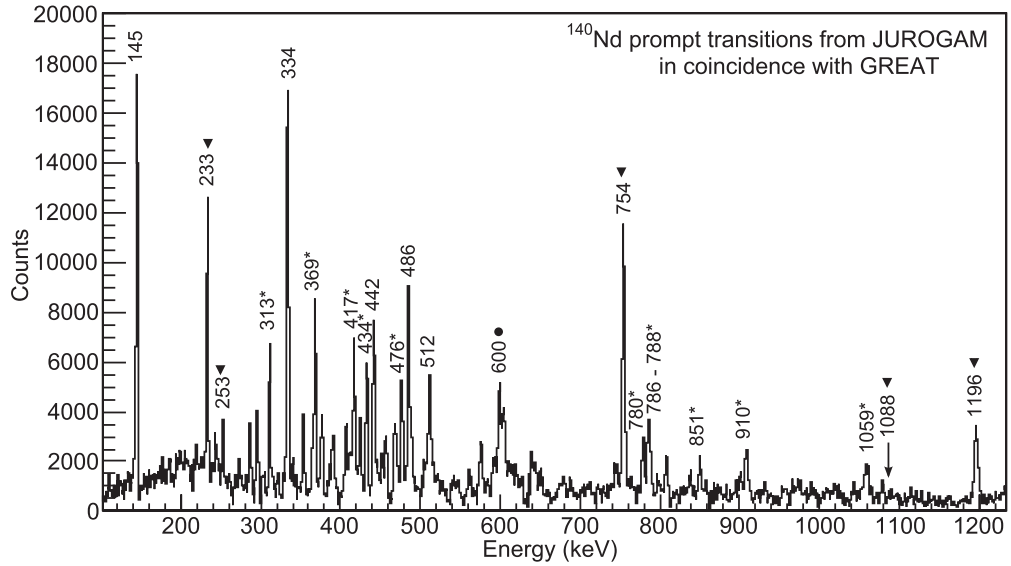


FIG. 5. Spectrum of prompt transitions measured by JUROGAM gated with selected clean transitions in $^{140}$Nd (188, 191, 506, 728, 868, and 1017 keV) measured by the clovers placed at the focal plane. The new transitions 233, 253, 714, 1196, and (1088) keV are indicated with a solid black triangle. The transitions marked with a star belong to Band 12. The 600-keV transition connecting Band 12 with the isomeric state is indicated with a solid black circle.

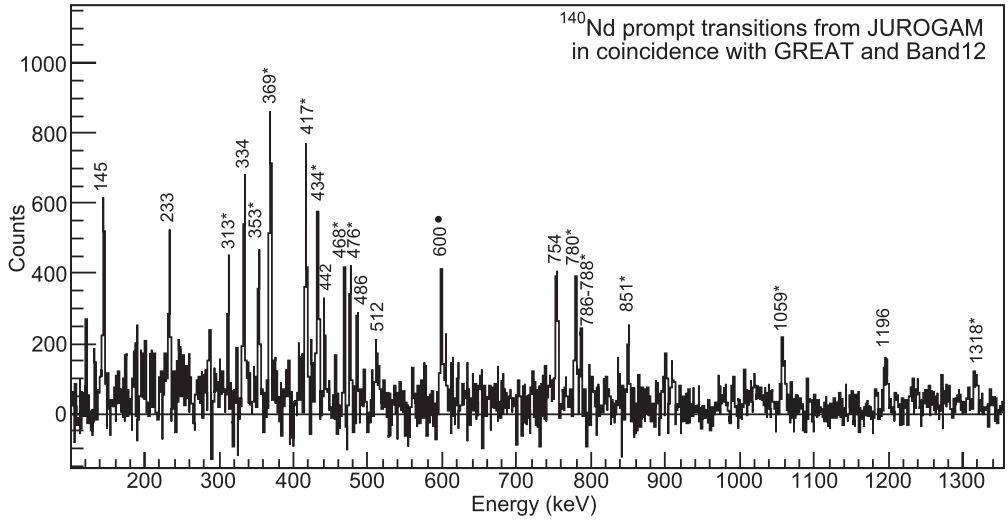


FIG. 6. Spectrum of prompt transitions measured by JUROGAM gated with selected transitions in $^{140}$Nd measured by the clovers placed at the focal plane and with the transitions above the spin 26 of Band 12 measured by JUROGAM. The transitions marked with a star belong to Band 12. The other transitions are the gamma rays coming from D3 and D4 bands and above isomer state connecting transitions. For the 600-keV transition, cf. Fig. 5 caption and Sec. III B1.

and very high angular momenta can be obtained from neutron excitations above the $N = 82$ shell gap into the $\nu f_{7/2}$, $\nu h_{9/2}$, and $\nu i_{13/2}$ orbitals.

### A. The low- and medium-spin configurations in $^{139}$Nd

The level scheme of $^{139}$Nd presents a very rich and complex structure at low and medium spins. We do not discuss here all the observed states at low and medium spins, because many of them have been already observed and discussed in Refs. [15–17] for $^{139}$Nd and in Refs. [2,8] for $^{140}$Nd.

The small deformation of $^{139}$Nd at low spins induces an ordering and occupation of the quasiparticle orbitals around the Fermi surface that is not much different from the spherical case. It is therefore natural to assume that the low-spin positive-parity states are based on configurations involving proton quasiparticle excitations within the $\pi(dg)$ subshell or neutron quasiparticle excitations within the $\nu(sd)$ or the $\nu h$ subshells. The low-spin negative-parity states involve either the $\pi(dg) \rightarrow \pi h$ proton excitations or the $\nu h \rightarrow \nu(sd)$ neutron excitations between the orbitals below the $N = 82$ magic shell closure.

The $23/2^+$ isomer has a $\nu[(h_{11/2})^{-2}(d_{3/2})^{-1}]$ configuration and is populated by transitions from three $25/2^-$ states. One can speculate therefore that the configurations of the three $25/2^-$ states involve the same neutron configuration of the $23/2^+$ isomer and 2 more nucleons from a broken pair, most likely 2 protons in the $\pi h_{11/2}$ and $\pi(d_{5/2}g_{7/2})$ orbitals. The presence of 1 $\pi(d_{5/2}g_{7/2})$ proton in the configuration of the $25/2^-$ states can explain the decay of the $25/2^-$ states to the $21/2^-$ and $23/2^-$ members of the $\nu h_{11/2}$ band, whose composition is $\nu h_{11/2} \otimes \pi(d_{5/2}g_{7/2})$.

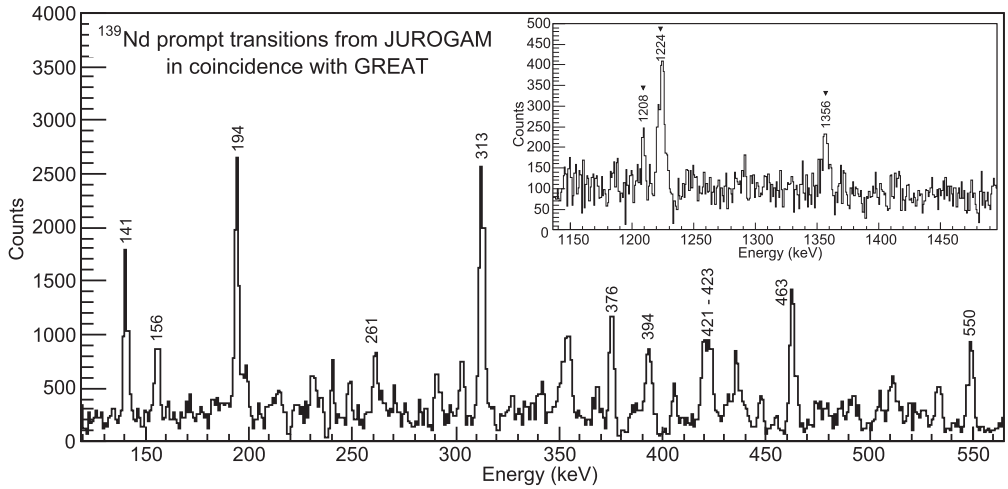


FIG. 7. Spectrum of prompt transitions measured by JUROGAM gated with the 605-, 665-, and 1071-keV transitions in $^{139}$Nd measured by the clovers placed at the focal plane. The transitions marked with a triangle are the new connecting transitions.

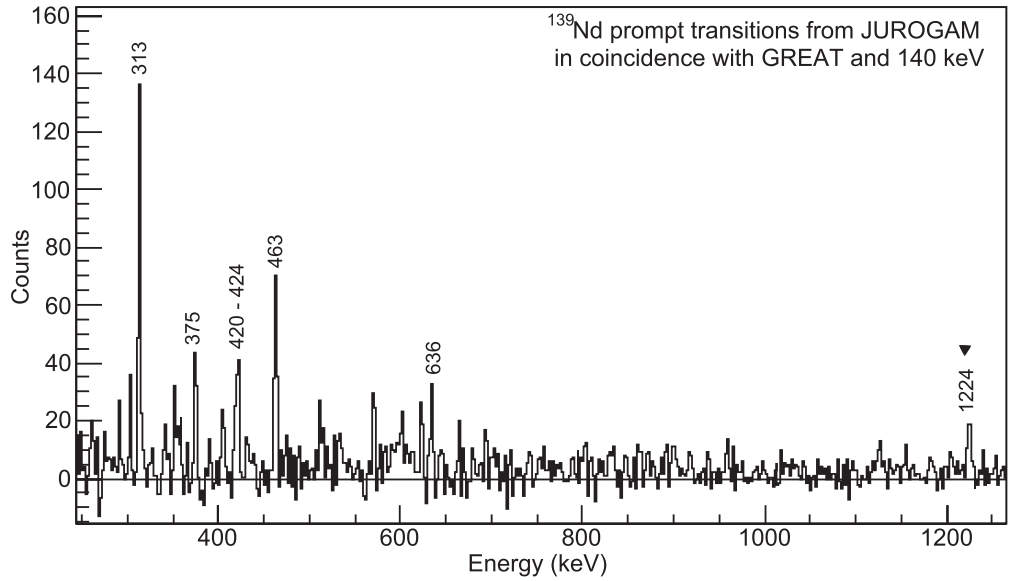


FIG. 8. Spectrum extracted from $\gamma$-$\gamma$ matrices of prompt events measured by JUROGAM gated with the 605-, 1071-, and 665-keV transitions in $^{139}$Nd measured by the clovers placed at the focal plane and by the JUROGAM transitions gated by the 140-keV transition. The transition marked with a triangle is a new one.

### B. The configurations of the high-spin dipole bands in $^{140}$Nd

The $20^+$ isomer of $^{140}$Nd has a maximum aligned configuration with 4 proton holes in the $\pi(dg)$ subshell and 2 neutron holes in the $\nu h_{11/2}$ subshell, i.e., a $\pi(dg)^4 \otimes \nu h^2$ configuration [8]. The $17^-$ state at 6404 keV is consistently interpreted as a $\pi(dg)^4 \otimes \nu h^1 d^1$ configuration. The newly observed transitions between bands D1 and D2 and the $20^+$ isomer have most probably a mixed $M1/E2$ character. This leads to positive parity for the two dipole bands. The most straightforward configuration that can be assigned to band D1 should include as building blocks part of the configurations of the states to which it is linked, in our case the $20^+$ and $17^-$ states. We propose therefore a $\pi h^2(dg)^2 \otimes \nu h^2$ configuration for band D1, which is obtained by the excitation of 2 protons from the $(dg)$ to the $h^2$ configuration. Such a configuration would also account for the bandhead spin of around 18, which can be obtained by a perpendicular coupling of the proton and neutron spins. It is more difficult to assign a configuration to band D2 for which only one transition is observed.

Band D3, which consists of strong dipole transitions and weak crossover transitions, is observed at an excitation energy higher by around 1.5 MeV above the $20^+$ isomer with an assigned 6-quasiparticle configuration $\pi(dg)^4 \otimes \nu h^2$, and around 1 MeV higher than band D1 for which we assigned

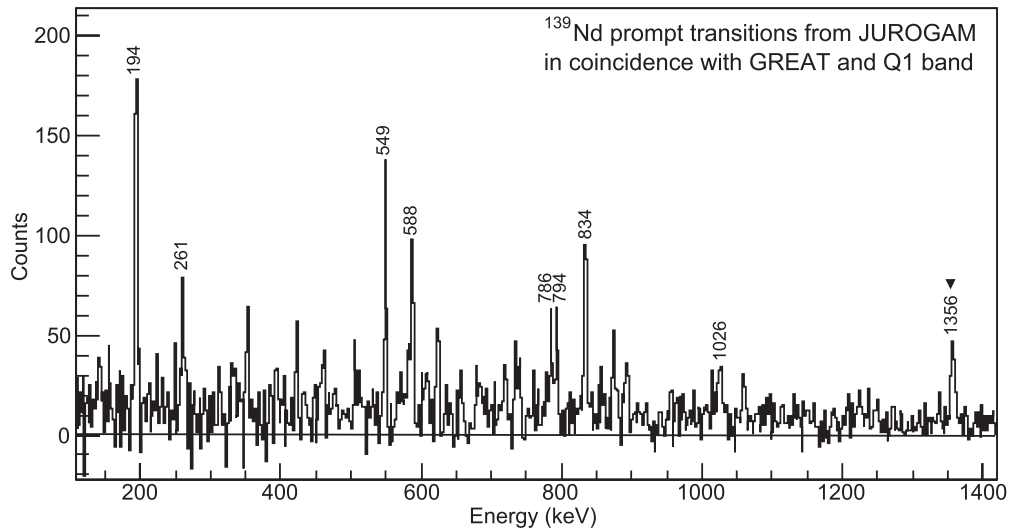


FIG. 9. Spectrum extracted from $\gamma$-$\gamma$ matrices of prompt events measured by JUROGAM gated with the 605-, 1071-, and 665-keV transitions in $^{139}$Nd measured by the clovers placed at the focal plane and by selected transitions detected by JUROGAM gated by 194-, 549-, and 834-keV transitions. The transition marked with a triangle is a new one.

the 6-quasiparticle configuration $\pi h^2(dg)^2 \otimes \nu h^2$. It could be based on a 6-quasiparticle configuration involving 2 more protons excited into the $\nu h_{11/2}$ subshell than band D1, having therefore a $\pi h^4 \otimes \nu h^2$ maximum aligned configuration.

## V. SUMMARY

The population of the high-spin isomers in $^{139}$Nd and $^{140}$Nd have been investigated using the reaction $^{96}$Zr($^{48}$Ca,$xn$) at a beam energy of 180 MeV and the JUROGAM + RITU + GREAT setup. The prompt-delayed coincidences between the $\gamma$ rays measured at the target position and at the focal plane of the RITU separator allowed the identification of several transitions linking known excited states in the two nuclei to the $23/2^+$ isomeric state in $^{139}$Nd and to the $20^+$ isomeric state in $^{140}$Nd. The newly observed transitions allowed the excitation energy of the $23/2^+$ isomer in $^{139}$Nd to be established. We assigned configurations to the bands connected to the isomers, getting a more coherent understanding of the multi-quasiparticle excitations at high spins in this mass region. The lifetimes of several isomers in $^{138}$Nd, $^{139}$Nd, $^{140}$Nd, and $^{136}$Ce were also measured, improving the accuracy of the lifetime values.

## ACKNOWLEDGMENTS

This work has benefited from the use of TNT2-D cards, developed and financed by CNRS/IN2P3 for the GABRIELA project. This work was partially financed by the EU through the EURONS project under Contract No. RII3 CT 2004 506065, by the Academy of Finland, and by the University of Jyväskylä within the Centre of Excellence program. We thank participating members of IPNO, CSNSM, and IRES for helping us. Warm thanks are addressed to the JYFL accelerator staff.

[1] C. M. Petrache, G. Lo Bianco, D. Ward, A. Galindo-Uribarri, P. Spolaore, D. Bazzacco, T. Kröll, S. Lunardi, R. Menegazzo, C. Rossi Alvarez, A. O. Macchiavelli, M. Cromaz, P. Fallon, G. J. Lane, W. Gast, R. M. Lieder, G. Falconi, A. V. Afanasjev, and I. Ragnarsson, Phys. Rev. C **61**, 011305(R) (1999).
[2] C. M. Petrache *et al.* Phys. Rev. C **72**, 064318 (2005).
[3] A. Neußer *et al.*, Phys. Rev. C **70**, 064315 (2004).
[4] S. Lunardi *et al.*, Phys. Rev. C **69**, 054302 (2004).
[5] C. M. Petrache, S. Frauendorf, M. Matsuzaki, R. Leguillon, T. Zerrouki, S. Lunardi, D. Bazzacco, C. A. Ur, E. Farnea, C. Rossi Alvarez, R. Venturelli, and G. de Angelis, Phys. Rev. C **86**, 044321 (2012).
[6] N. Yoshikawa, Nucl. Phys. A **243**, 143 (1975).
[7] J.-C. Merdinger, F. A. Beck, E. Bozek, T. Byrski, C. Gehringer, Y. Schutz, and J.-P. Vivien, Nucl. Phys. A **346**, 281 (1980).
[8] C. M. Petrache, R. A. Bark, S. T. H. Murray, M. Fantuzi, E. A. Lawrie, S. Lang, J. J. Lawrie, S. M. Maliage, D. Mengoni, S. M. Mullins, S. S. Ntshangase, D. Petrache, T. M. Ramashidzha, and I. Ragnarsson, Phys. Rev. C **74**, 034304 (2006).
[9] M. Ferraton, R. Bourgain, C. M. Petrache, D. Verney, F. Ibrahim, N. de Séréville, S. Franchoo, M. Lebois, C. Phan Viet, L. Sagui, I. Stefan, J. F. Clavelin, and M. Vilmay, Eur. Phys. J. A **35**, 167 (2008).
[10] P. Rahkila, Nucl. Instrum. Methods Phys. Res., Sect. A **595**, 637 (2008).
[11] O. Stezowski, http://agata.in2p3.fr/gw/doxy.
[12] D. C. Radford, Nucl. Instrum. Methods Phys. Res., Sect. A **361**, 297 (1995).
[13] D. C. Radford, Nucl. Instrum. Methods Phys. Res., Sect. A **361**, 306 (1995).
[14] M. Müller-Veggian, H. Beuscher, R. M. Lieder, Y. Gono, D. R. Haenni, A. Neskakis, and C. Mayer-Böricke, Z. Phys. A **290**, 43 (1979).
[15] S. Bhowal *et al.*, Phys. Rev. C **84**, 024313 (2011).
[16] S. Kumar, R. Palit, H. C. Jain, I. Mazumdar, P. K. Joshi, S. Roy, A. Y. Deo, Z. Naik, S. S. Malik, and A. K. Jain, Phys. Rev. C **76**, 014306 (2007).
[17] Q. Xu, S. J. Zhu, X. L. Che, J. G. Wang, H. B. Ding, L. Gu, L. H. Zhu, X. G. Wu, Y. Liu, C. Y. He, and G. S. Li, Phys. Rev. C **78**, 034310 (2008).